DOI 10.1002/prca.200800167 *Proteomics Clin. Appl.* 2009, *3,* 30–40

RESEARCH ARTICLE

Proteomic analysis of breast cancer tissue reveals upregulation of actin-remodeling proteins and its relevance to cancer invasiveness

Dong-Hyun Kim[1], Jinhee Bae[2]*, Jong Won Lee[3], Seon-Young Kim[4], Yong-Hak Kim[1], Ji-Yeon Bae[3], Jae Kyo Yi[3], Myeong-Hee Yu[1], Dong-Young Noh[3]** and Cheolju Lee[2]*

[1] Functional Proteomics Center, Korea Institute of Science and Technology, Seoul, Korea
[2] Life Sciences Division, Korea Institute of Science and Technology, Seoul, Korea
[3] Cancer Research Institute, Seoul National University College of Medicine, Seoul, Korea
[4] Medical Genomics Research Center, Korea Research Institute of Bioscience and Biotechnology, Daejeon, Korea

Received: July 27, 2008
Revised: September 24, 2008
Accepted: September 29, 2008

There is an emerging interest in protein expression profiling with the aim of identifying novel diagnostic markers and therapeutic targets in breast cancer. We analyzed breast cancer tissues by 2-D DIGE using a narrow range IPG strip (pH 5.5–6.7) after the immunodepletion of serum albumin and Ig. Sixty-three protein spots were detected with more than ±1.8-fold differences ($p < 0.05$ for three technical replicates) from a set of tissue samples in which three tumor and three nontumor samples were randomly selected from six breast cancer subjects and pooled separately. Of these, 53 proteins were successfully identified by MS. Among the proteins whose levels were increased, we identified three novel WD-repeat-motif-bearing proteins that have been known to be involved in actin remodeling: Arp2/3 complex subunit 2 (p34-Arc), coronin-1A and WD-repeat protein 1 (Wdr1). Significantly increased amounts of p34-Arc and coronin-1A in breast cancer were also shown by Western blot analysis of matched tumor and nontumor tissue samples ($N = 11$, $p < 0.05$), and were consistent with the mRNA levels retrieved from publicly available microarray databases. The siRNA knockdown of p34-Arc attenuated the invasion of SK-BR3 breast cancer cells into Matrigel. In contrast, the overexpression of coronin-1A increased this invasive activity. Taken together, the cellular levels of p34-Arc and coronin-1A were linked to cancer development and migration. The data obtained from the present study provides new insight into the management of breast cancer.

Keywords:
Arp2/3 complex subunit 2 / Breast cancer / Coronin-1A / DIGE / Invasion assay

Correspondence: Dr. Cheolju Lee, Life Sciences Division, Korea Institute of Science and Technology, 39-1 Hawolgok, Seongbuk, Seoul 136-791, Korea
E-mail: clee270@kist.re.kr
Fax: +82-2-958-6919

Abbreviations: ER, estrogen receptor; **Her2,** C-erb2; **LCM,** laser capture microdissection; **p34-Arc,** Arp2/3 complex subunit 2; **PR,** progesterone receptor; **Wdr1,** WD-repeat protein 1

1 Introduction

Breast cancer is one of the leading causes of death in women worldwide, accounting for more than 400 000 deaths *per* year (eMedicine, http://www.emedicine.com/rc/rc/i29/

* Both these authors contribute equally to this work.
** Additional corresponding author: Dr. Dong-Young Noh; E-mail: dynoh@snu.ac.kr

breastcancer.htm). In spite of major advances in the areas of detection and treatment, a considerable number of breast cancers are detected during the late stages of tumor development. This underscores the need to discover new biological markers or targets for the early detection and management of breast cancer [1]. Breast cancer is a complex disease during which the accumulation of numerous molecular alterations causes genetic instability, cell proliferation, and acquisition of an increasingly invasive and resistant phenotype [2, 3]. Since the molecular character of each breast cancer is different and of diverse origin, prognostication, and management of breast cancer can be significantly improved by using multiple markers. This has lead to an emerging interest in protein expression profiling with the aim of identifying novel diagnostic markers and therapeutic targets.

Proteomic strategies have been used to identify cancer-specific protein markers. It is apparent from a number of reports that 2-DE in combination with MS is a basic technology to separate proteins and compare their expression levels quantitatively [4]. However, conventional 2-DE has a drawback in that the number of protein spots and the level of protein expression vary between gels even between identical samples. The 2-D DIGE has been developed to simplify the analysis and comparison of protein expression by two or three samples distinguished in a single gel [5, 6].

To identify and evaluate cancer-related proteins, tumor tissues, blood plasma, or secreted body fluids such as urine, tears, sweat, and saliva, are used as a source of the proteome. A tumor tissue is the most reliable source to identify new cancer-specific proteins, based on the full clinical and histological records of the cancer subjects. Since there are individual variations that can affect uncertainties in response to new markers or targets, it is important to know whether the samples are randomized or matched sets of tumor and nontumor tissues. The degree of neovascularization increases as breast tumor progresses [7] and therefore plasma proteins can often interfere with the analyses of breast tissue proteomes. Laser capture microdissection (LCM) is an effective method of eliminating such interferences [8, 9]. In spite of such an advantage, this method is still laborious and the amount of resultant proteins is very limited.

The object of this study was to identify breast cancer-specific proteins using 2-D DIGE. Circulating blood is likely to contaminate cancer tissues, and the abundant proteins in blood serum may strongly interfere with the spot signals of tissue proteins. To achieve a robust and sensitive detection of low abundance proteins, a pool of tumor, and nontumor tissue samples randomly chosen from a tissue archive must be depleted of albumin and Ig. High resolution in protein separation is achieved by the use of a narrow range IPG strip (pH 5.5–6.7) rather than one with a broader pH range. A cancer-specific protein identified by MS can be further evaluated by immunological tests on matched tumor and nontumor tissue samples, analysis of the gene expression in the Breast Cancer Microarray datasets, and knockdown or overexpression of the gene in a breast cancer cell line. Our *in vitro* study on breast cancer cells showed that the cellular levels of actin-remodeling Arp2/3 complex subunit 2 (p34-Arc) and coronin-1A were positively related to the invasive activity and migration of the cell.

2 Materials and methods

2.1 Tissue samples and cell lines

Breast cancer tissues were obtained from the frozen tissue archives in the Breast Care Center of Seoul National University Hospital. Authorization for the use of these tissues for research purposes was obtained from the Institutional Review Board of Seoul National University Hospital. The clinical records of patients, such as age at diagnosis, histology, tumor size, and lymph node status, were reviewed to select proper tissue samples as given in Table 1. Immunohistochemical analysis for the expression of estrogen receptor (ER), progesterone receptor (PR), and C-erb2 (Her2) was performed as described previously [10]. All the tumor samples used contained more than 50% tumor cells, and stored at −80°C before use. Three tumor samples and three nontumor samples were randomly chosen from the tissue archive, and pooled separately. Eleven pairs of matched tumor and nontumor samples were tested to evaluate cancer-specific proteins by Western blot. In total, tissue samples from 17 cancer subjects, 6 for initial screening, and 11 for the subsequent validation, were used in this study.

Five human breast cancer cell lines (MCF7, Hs578T, SK-BR-3, MDA-MB-231, and ZR-75-1) were obtained from American Type Culture Collection (Manassas, VA, USA) or Korean Cell Line Bank (Seoul, Korea). SK-BR-3 and ZR-75-1 were grown in RPMI 1640 (Gibco® Cat. no. 11875-093; GIBCO BRL, Grand Island, MD, USA) supplemented with 10% v/v FBS (GIBCO BRL), 100 units/mL penicillin and 100 μg/mL streptomycin. MDA-MB-231 cell was grown in DMEM (Gibco Cat. no. 11995-065) with the same supplements, and Hs578T and MCF7 were cultured in the same media to which 0.01 mg/mL insulin (Sigma–Aldrich, St. Louis, MO, USA) was added. All the cell lines were cultured at 37°C in a humidified incubator with a mixture of 95% air and 5% CO_2.

2.2 Preparation of tissue proteome

The frozen tissues were pulverized with liquid nitrogen in a mortar. The resultant tissue powder was washed with PBS, and sonicated in 10 mM Tris-HCl buffer (pH 7.4) containing a protease inhibitor cocktail (Roche, Mannheim, Germany). The cell debris was removed by centrifugation at $14\,000 \times g$ for 10 min, and the supernatant was transferred to a microcentrifuge tube. HSA and IgG were then removed using a Vivapure Anti-HSA/IgG kit according to the manufacturer's protocol (Sartorious group, Goettingen, Germary).

Table 1. Characterization of breast tissues used in this experiment

Experiment	Case no.	Age	Histology	*T*	*N*	*M*	Stage	ER/PR	Her2	Tissue type
DIGE	1	50	Infiltrating duct carcinoma	1	0	0	I	−/−	0	Nontumor
	2	51	Infiltrating duct carcinoma	2	0	0	IIA	−/−	3+	Nontumor
	3	60	Infiltrating duct carcinoma	2	2	0	IIIA	−/−	1+	Nontumor
	4	60	Infiltrating duct carcinoma	1	0	0	I	−/−	0	Tumor
	5	59	Infiltrating duct carcinoma	2	0	0	IIA	−/−	0	Tumor
	6	64	Infiltrating duct carcinoma	2	0	0	IIA	−/−	0	Tumor
Western blot	1	45	Infiltrating duct carcinoma	2	1	0	IIB	−/+	2+	Pair (tumor/nontumor)
	2	45	Infiltrating duct carcinoma	2	0	0	IIA	−/−	2+	Pair (tumor/nontumor)
	3	30	Infiltrating duct carcinoma	2	0	0	IIA	−/−	0	Pair (tumor/nontumor)
	4	30	Infiltrating duct carcinoma	3	3	0	IIIC	−/−	0	Pair (tumor/nontumor)
	5	40	Infiltrating duct carcinoma	2	0	0	IIA	−/−	3+	Pair (tumor/nontumor)
	6	60	Infiltrating duct carcinoma	2	0	0	IIA	−/−	3+	Pair (tumor/nontumor)
	7	61	Infiltrating duct carcinoma	1	1	0	IIA	−/−	0	Pair (tumor/nontumor)
	8	72	Infiltrating duct carcinoma	2	0	0	IIA	−/−	1+	Pair (tumor/nontumor)
	9	73	Infiltrating duct carcinoma	2	2	0	IIIA	−/−	1+	Pair (tumor/nontumor)
	10	84	Infiltrating duct carcinoma	2	0	0	IIA	+/+	1+	Pair (tumor/nontumor)
	11	86	Infiltrating duct carcinoma	2	1	0	IIB	−/−	0	Pair (tumor/nontumor)

Three parameters of TNM classification for each breast tumor are defined: *T*, size or direct extent of the tumor; *N*, degree of spread to regional lymph nodes; *M*, presence of metasis. Results of ER/PR are defined as positive for nuclear staining of ≥10% tumor cells. Her2 expression is determined by the membranous staining of tumor cells and scored as 0 for negative staining, 1+ for weak staining, 2+ for moderate staining, and 3+ for strong staining in at least 10% of tumor cells.

2.3 2-D DIGE

The immunodepleted tissue lysate was diluted into 100 μL of 2-DE buffer (7 M urea, 2 M thiourea, 30 mM Tris, 5 mM magnesium acetate, 4% CHAPS, 1% NP-40, pH 8.5) and incubated at 24°C for 30 min with intermittent shaking. The protein concentration was determined by the micro-Bradford assay (BioRad Laboratories, Hercules CA, USA). Equal amounts of proteins from three tumor samples and three nontumor samples were pooled separately (Table 1), and each 150 μg of the pooled samples was labeled with 1.2 nmol of Cy3 for nontumor, Cy5 for tumor, or Cy2 for internal standard (1:1 mixture of nontumor and tumor) according to the manufacturer's guideline (GE Healthcare, Uppsala, Sweden). The mixture of differently Cy-labeled samples was split into three parts and resolved by the first dimensional electrophoresis on narrow range IPG strips (pH 5.5–6.7, 24 cm) using an IPGphor IEF system. The second dimensional electrophoresis was carried out on 12.5% SDS polyacrylamide gels (24 cm × 24 cm) using an Ettan Dalt 6 system.

The three 2-D DIGE gel images were scanned on a Typhoon 9400 variable mode imager (GE Healthcare). Proteins in different level were detected from normalized spot volumes by using the DIA module of DeCyder and statistically significant differences ($p < 0.05$) were analyzed by *t*-test in the BVA module. All protein spots in DIGE gels were thereafter visualized by the silver-staining method.

2.4 Protein digestion and MS

Differentially expressed protein spots were manually excised from gels, and in-gel digested with 8 ng/μL trypsin (Promega, Madison, WI, USA) as described elsewhere [11]. The recovered tryptic peptides were analyzed by MS using an AB 4700 Proteomics Analyzer (Applied Biosystems, Framingham, MA, USA) in both MS and MS/MS modes. The mass spectrometer was set to acquire positive ion MS survey scans over the mass range of 700–3500 Da. Once the MS survey scans were completed, the data were processed to generate a list of precursor ions for interrogation by MS/MS. Air was used as the collision gas at a pressure of 1.4×10^{-6} torr in the MS/MS mode. The instrument was equipped with an Nd:YAG laser (PowerChip, JDS Uniphase, San Jose, CA, USA) operating at 200 Hz and controlled by Applied Biosystems Explorer version 1.1 software. The mass resolution of the instrument was 15 000 and 4000 in the MS and MS/MS modes, respectively. The mass accuracy in the MS mode was roughly ±30 ppm, while in the MS/MS mode, the mass accuracy was ±50 ppm.

Protein identification was attempted by MS/MS ion search (mass tolerance for precursor ion, 100 ppm; fragment ion, 0.5 Da) based on the tandem mass spectrometric data from at least two peptides to interrogate the Swiss-Prot protein database (release 54.7, 333 445 sequences) using MASCOT (version 1.9, MatrixScience, London, UK). Searches were performed with the options

of a fixed modification of carbamidomethylation at cysteine and a maximum of one missed trypsin cleavage. The automatic data analysis and database searches were achieved using GPS Explorer™ version 3.5 (Applied Biosystems). Protein total ion scores of greater than 75 were considered to be statistically significant ($p < 0.05$). If there was no reliable MS/MS spectrum (MASCOT score<30), protein identification was attempted by PMF. Each raw spectrum was opened in Data Explorer™ (version 4.6, Applied Biosystems) software and less than 40 top mass peaks were selected by S/N threshold setting and then treated with advanced base-line correction. The spectrum was calibrated with more than two peptides resulting from trypsin autolysis (m/z 842.5100, 2211.1046, and 2283.1807). Peak list of monoisotopic masses was searched against Swiss-Prot database (release 54.7, 333 445 sequences) using the following parameters: trypsin as enzyme, one possible missed cleavage, peptide tolerance of 20 ppm, and a fixed modification of carbamidomethylation at cysteine. A hit was considered to be significant if the scores obtained for PMF and MS/MS data clearly exceeded the significance threshold ($p < 0.05$).

2.5 Western blot

HSA/IgG-depleted tissue samples ($N = 11$ pairs of matched tumor and nontumor) were analyzed by 10% SDS-PAGE, and electrotransferred onto PVDF membranes using the Mini Trans-Blot® cell (BioRad Laboratories). The membranes were serially probed with the following primary antibodies: anti-p34-Arc (1:500, Millipore, Billerica, MA, USA), anti-coronin-1A (1:2500, Abnova Corporation, Taipei, Taiwan), and anti-actin (1:2000, Sigma–Aldrich Chemie, Taufkirchen, Germany). A donkey antirabbit IgG HRP (1:4000, GE Healthcare) or a sheep antimouse IgG horseradish peroxidase (1:1000, GE Healthcare) in TBS-Tween 20 buffer was used as the secondary antibodies. The chemiluminescence was developed using ECL™ Western Blotting Detection (GE Healthcare).

2.6 Transfection and siRNA

The coronin-1A gene cloned into plasmid pCNS-D2 was obtained from the Genome Research Center at Korea Research Institute of Bioscience and Biotechnology (Daejeon, Korea). The siRNA duplexes targeted for p34-Arc were constructed with the following sequences at Bioneer (Seoul, Korea): sense (5′-GAC GAU GUG GUC AUU GGA A(dTdT)-3′); antisense (5′-UUC CAA UGA CCA CAU CGU C(dTdT)-3′). The siRNA knockdown of p34-Arc and the overexpression of coronin-1A by the plasmid transfection in breast cancer cell lines were performed using Lipofectamine™ 2000 according to the manufacturer's protocol (Invitrogen, Carlsbad CA, USA). At 72 h after transfection of p34-Arc siRNA or at 24 h after transfection of coronin-1A plasmid, the cells were harvested using TNN buffer containing 20 mM Tris-HCl (pH 7.5), 150 mM NaCl, 0.5% NP-40, 10% glycerol, and protease inhibitor cocktail (Roche) for subsequent cell invasion assay and Western blot analysis.

2.7 Cell invasion assay

Effects of coronin-1A or p34-Arc on the invasive activity of breast cancer cells were determined by using a transwell chamber system with an 8 μm polycarbonate filter (Costar Corning, Acton, MA, USA). The lower and upper sides of the filter were coated with gelatin and matrigel, respectively. Breast cancer cell lines were harvested by trypsinization at 72 h after the transfection of p34-Arc siRNA or at 24 h after transfection of coronin-1A plasmid. The cells (8×10^4) suspended in serum-free RPMI containing 0.1% v/v BSA were placed to the upper chamber of the transwell, and RPMI supplemented with 10% v/v FBS was placed into the lower chamber. After 16 h incubation of the transwell system at 37°C, the cells migrated through the filter were fixed with methanol, stained with HE, and their number was counted.

3 Results and discussion

3.1 Optimization of gel electrophoresis

In order to identify proteins associated with breast cancer development, we compared 2-D gel patterns of tumor and nontumor tissue proteomes. Three tumor samples and three nontumor samples were randomly selected from a tissue archive as a training set for robust identification of cancer-specific proteins by 2-D DIGE without consideration of individual variations. These samples were pooled separately, and then triplicated for the purpose of technical replication in gel electrophoresis. Nontumor tissue samples were obtained from more than 5 cm away from the tumor margin of the breast cancer. The samples were immunodepleted of serum albumin and IgG, and applied to a narrow range IPG strip (pH 5.5–6.7). Since breast tissue is rich in circulating blood [7], the immunodepletion process was helpful for minimization of sample bias (Supporting Information Fig. 1). A narrow range IPG strip was used because of its suitability for higher resolution in protein separation than a broad range strip. In addition, protein spots at a pI of about 5.5 and having a molecular weight of 67 kDa were excluded from the image analysis in order to reduce normalization bias that stemmed from incompletely depleted serum albumin.

3.2 Analysis of differentially expressed proteins by 2-D DIGE

The above conditions were suitable for comparison of protein profiles of tumor and nontumor tissue samples by 2-D DIGE. The 2-D DIGE is not only effective to reduce the gel-to-gel variability associated with conventional 2-DE, but also improves the accuracy of quantitative protein profiling [12,

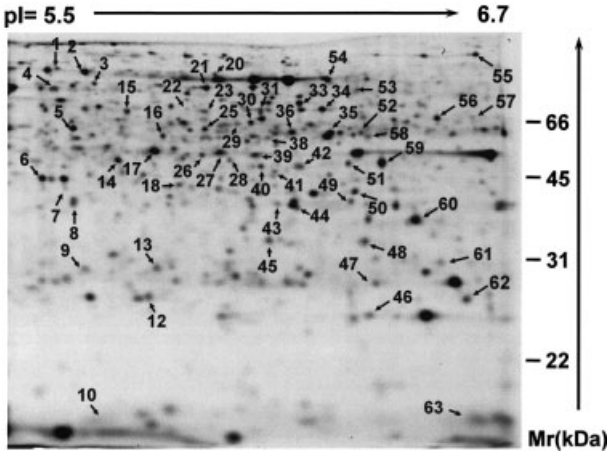

Figure 1. 2-DE map for the proteome obtained from breast cancer tissues. The original DIGE image in Supporting Information Fig. 2 was reprocessed into gray-scale picture. Differentially expressed proteins that were identified by following MS are marked with numbered arrows.

13]. Figure 1 shows a typical 2-D DIGE gel image. About 500 protein spots were detected, and 63 spots were identified as differentially expressed with significant changes of more than ±1.8-folds ($p < 0.05$). Of these proteins, 53 of them were successfully identified by MS, as summarized in Table 2, among which 38 proteins were expressed to a greater extent in the tumor sample than the nontumor sample. Only 15 proteins were expressed to a lower extent in the tumor sample than the nontumor sample. Among the identified proteins, catalase [14], malate dehydrogenase [15], isocitrate dehydrogenase [16], elongation factor Tu [17, 18], heat-shock protein 27 [19], and moesin [20] have previously been shown to be related to breast cancer. This indicated that our 2-D DIGE data of differential protein expression in breast cancer was reliable and comparable to previous studies [14–16, 18–21].

3.3 Actin remodeling proteins are upregulated in cancer tissues

Three upregulated proteins were identified as coronin-1A (spot no. 30), Arp2/3 complex 34 kDa subunit 2 (p34-Arc, no. 48), and WD-repeat protein 1 (Wdr1, no. 33). The spots showed expected mass profiles that were well matched with the theoretical values for the tryptic digests of corresponding proteins (Fig. 2, Table 2). False discovery due to sample contamination by blood proteins was ruled out, since all three proteins were increased in the tumor sample, in comparison to serum albumin and serotransferin, which exist predominantly in serum and showed negative ratio values (Table 2). However, we cannot ignore the possibility that inflammatory cells accumulating during the progression of invasive ductal breast cancer or tissue interstitial fluid may affect the analysis.

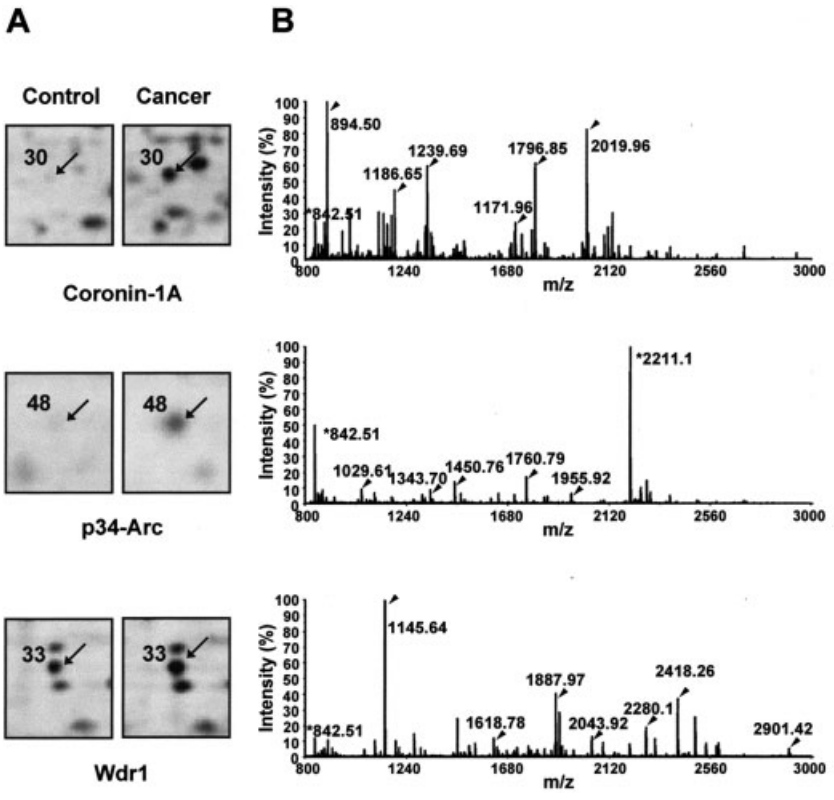

Figure 2. (A) 2-DE images for coronin-1A, p34-Arc, and Wdr1. Numbers indicate spot numbers as in Fig. 1. (B) MALDI-TOF mass spectra of tryptic digests of coronin-1A, p34-Arc, and Wdr1. Arrowheads indicate peptide mass peaks matched to the identified proteins. Asterisks indicate autolytic product of trypsin which were used as internal standard to calibrate the mass spectra in PMF.

Table 2. List of proteins identified as differentially expressed in breast cancer tissues

No.[a]	Protein	Ratio (-fold)[b]	*t*-Test *p*-value[c]	Swiss-Prot accession no.	MW (kDa)	p*I*	ID method	Sequence coverage	MASCOT score	No. of matched peptide
1	Gelsolin	−9.1	0.006	P06396	85.7	5.9	MS	21	111	11
2	Gelsolin	4.7	0.039	P06396	85.7	5.9	MS	14	67	8
3	Glycyl-tRNA synthetase	5.1	0.011	P41250	83.1	6.6	MS	27	118	13
4	Serum albumin	−6.0	0.002	P02768	69.4	5.9	MS	19	96	10
5	Tryptophanyl-tRNA synthetase	8.4	0.002	P23381	53.2	5.8	MS/MS	38	206	14
6	Macrophage capping protein	8.1	0.007	P40121	38.5	5.9	MS	27	89	7
7	60S acidic ribosomal protein P0	3.7	0.011	P05388	34.3	5.7	MS	25	57	5
8	60S acidic ribosomal protein P0	3.5	0.042	P05388	34.3	5.7	MS	29	58	5
9	Heat-shock protein β-1	4.8	0.022	P04792	22.8	6.0	MS	32	72	6
10	Fatty acid-binding protein, adipocyte	−4.7	0.010	P15090	14.6	6.8	MS	31	57	4
12	Proteasome subunit β type 3	2.1	0.003	P49720	22.9	6.1	MS	38	78	6
13	ER protein ERp29	2.2	0.011	P30040	29.0	6.8	MS	19	47	4
14	Adenosylhomocysteinase	2.1	0.042	P23526	47.6	5.9	MS	32	107	15
15	Serum albumin	−5.7	0.026	P02768	69.4	5.9	MS	21	119	11
16	T-complex protein 1 subunit β	3.9	0.025	P78371	57.4	6.0	MS	37	182	14
17	Rab GDP dissociation inhibitor β	3.8	0.02	P50395	50.7	6.1	MS/MS	19	129	5
18	Actin-like protein 2	5.0	0.004	P61160	44.8	6.3	MS	19	57	5
20	Serotransferrin	−5.7	0.004	P02787	77.0	6.8	MS	27	186	16
21	Moesin	4.6	0.018	P26038	67.7	6.1	MS	26	174	15
22	Dihydropyrimidinase-related protein 2	−3.3	0.033	Q16555	62.3	6.0	MS	21	60	7
25	PRP19/PSO4 homolog	3.9	0.015	Q9UMS4	55.2	6.1	MS	30	129	11
27	Elongation factor 1-γ	4.5	0.016	P26641	50.0	6.3	MS/MS	10	114	3
28	Probable ATP-dependent RNA helicase DDX48	6.0	0.001	P38919	46.9	6.3	MS	28	113	12
29	Retinal dehydrogenase 1	−2.5	0.008	P00352	54.7	6.3	MS	21	79	8
30	Coronin-1A	5	0.002	P31146	51.7	6.3	MS/MS	18	154	7
31	T-complex protein 1 subunit zeta	2.9	0.042	P40227	57.9	6.3	MS	18	66	7
33	WD repeat-containing protein1	2.5	0.035	O75083	66.7	6.2	MS/MS	24	593	9
34	Stress-induced phosphoprotein 1	2.8	0.017	P31948	62.6	6.4	MS	35	218	20
35	Cytosol aminopeptidase	3.3	0.008	P28838	52.6	6.3	MS/MS	22	241	8
36	Retinal dehydrogenase 1	−2.5	0.002	P00352	54.7	6.3	MS/MS	13	113	6
38	Fibrinogen β chain	−6.5	0.007	P02675	55.9	8.5	MS	36	179	14
39	α-Enolase	1.8	0.045	P06733	47.0	7.0	MS	18	70	6
40	α-Centractin	2.4	0.028	P61163	42.6	6.2	MS/MS	10	77	2
41	Adenosine kinase	3.1	0.007	P55263	40.5	6.2	MS	17	52	5
42	Glutamine synthetase	3.8	0.005	P15104	41.9	6.4	MS	23	69	7
44	Annexin A1	9.4	0.020	P04083	38.6	6.6	MS	43	155	11
45	Purine nucleoside phosphorylase	3.6	0.006	P00491	32.1	6.5	MS	54	141	10
46	Proteasome subunit β type 2	2.4	0.026	P49721	22.8	6.5	MS	38	79	6
47	Triosephosphate isomerase	−1.8	0.022	P60174	26.5	6.5	MS	38	91	7
48	Actin-related protein 2/3 complex subunit 2	2.6	0.003	O15144	34.3	6.8	MS	31	152	11
50	Sialic acid synthase	2.3	0.036	Q9NR45	40.3	6.3	MS	18	64	6
51	Elongation factor Tu, mitochondrial	3.9	0.039	P49411	49.5	7.3	MS	24	89	8
53	GMP synthase (glutamine-hydrolyzing)	3.1	0.034	P49915	76.7	6.4	MS	30	180	15
54	Serotransferrin	−5.7	0.001	P02787	77.0	6.8	MS	27	162	14
55	Elongation factor 2	8.7	0.009	P13639	95.2	6.4	MS	26	225	20
56	Dihydrolipoyl dehydrogenase, mitochondrial	3.2	0.018	P09622	54.2	7.6	MS	21	108	10
57	Catalase	−3.3	0.000	P04040	59.6	7.0	MS	28	113	10
58	Fibrinogen β chain	−9.3	0.007	P02675	55.9	8.5	MS	49	308	22
59	Isocitrate dehydrogenase [NADP] cytoplasmic	2.4	0.031	O75874	46.7	6.5	MS	42	179	14
60	Malate dehydrogenase, cytoplasmic	2.2	0.028	P40925	36.3	6.9	MS/MS	16	73	3
61	Carbonic anhydrase 1	−14.0	0.001	P00915	28.7	6.6	MS/MS	37	282	6
62	Proteasome subunit α type 2	2.3	0.028	P25787	25.8	7.1	MS	43	110	7
63	Hemoglobin β chain	−12.3	0.003	P68871	15.9	6.8	MS/MS	32	105	4

Detailed information of identified peptide sequences are shown in Supporting Information Table 1.

a) Spot numbers are indicated in Fig. 1.

b) "+" and "−" indicate the factor increase or decrease in spot intensity of tumor tissue relative to the nontumor control.

c) *p*-values of student's *t*-test between tumor and nontumor tissue samples in triplicate gels.

The three proteins identified, were classified into the functional group of cell growth and maintenance. They contain consecutive WD-repeat motifs at their N-termini and a leucine zipper domain at the C-termini, which is involved in interaction with actin. Wdr1 is synonymously called actin-interacting protein 1, and functions as a unique regulator of ADF/cofilin that enhances actin depolymerization, filament fragmentation, and promotes reorganization of the filaments in the presence of ADF/cofilin [22].

Another protein, p34-Arc is one of seven subunits of the Arp2/3 complex that is strongly concentrated in the earliest aggregation of F-actin formed in response to growth factors [23], and that creates Y-shaped junctions on existing filaments resulting in branched actin networks [24, 25]. Nucleation-promoting factors like the Wiskott–Aldrich syndrome protein (WASP) family integrate multiple upstream signals to induce actin polymerization through the Arp2/3 complex, which increases the cell protrusive activity associated with cell migration and invasion [24, 25].

Coronin-1A is known to mediate actin dynamics in a variety of processes [26], and is found abundantly in lymphocytes and macrophages [27]. Coronins that bind to filamentous actin and Arp2/3 complex are involved in modulating actin dynamics [26, 27]. Though little is yet known about its relation to cancer, the coronin family of proteins are essential in cell motility since the knockdown of coronin-1B by shRNA decreased the motility of Rat2 cells [28].

Actin remodeling is important for cancer development. Several studies have shown that the expression of some actin monomers was increased in cancer tissues [29, 30]. Furthermore, actin remodeling is especially active in pseudopodium or lamellipodium when tumor cells invade surrounding epithelial cells and undergo metastasis [31]. We thus tested the possibility of using actin-interacting proteins, Wdr1, p34-Arc, and coronin-1A, as potential breast cancer markers.

3.4 Transcriptomics reveals upregulations of coronin 1A and p34-Arc in breast cancer

To investigate whether the mRNA levels of coronin-1A, p34-Arc, and Wdr1 changed in a similar pattern to their protein levels in breast cancer, four gene expression datasets were downloaded from the Gene Expression Omnibus (GEO) database (http://www.ncbi.nlm.nih.gov/projects/geo/). The datasets included GSE1456 [32], GSE2034 [33], GSE3193 [34], and GSE3494 [35]. GSE3193 was made up from dual channel cDNA arrays and the others from single channel Affymetrix U133A platforms. To analyze the cDNA datasets, the missing values (≥30%) were initially filtered out and imputed by the k-nearest neighbor method using a GEPAS web server [36]. The average values of gene expression were calculated from replicate probes. Then, the mean of included normal samples was subtracted from the value of each tumor sample. To analyze the Affymetrix datasets, the expression values computed by MAS5 algorithms were consistently used to ensure similar processing, and were normalized by a global mean method to a target density of 500. Each value was log 2-transformed and the mean expression value of breast nontumor tissue samples including GSM44683, GSM158644, GSM158645, GSM158646, GSM152336, and GSM152337 was subtracted from each transformed value. As shown in Table 3, breast cancer significantly increased the gene expression of coronin-1A (2–10-folds, $p < 0.05$) and p34-Arc (1.5–2-folds, $p < 0.05$) in tumor tissues. In contrast, Wdr1 did not show any significant change at the mRNA level ($p > 0.05$).

Table 3. Increased mRNA levels of coronin-1A and p34-Arc in breast cancer tissues

Dataset	Coronin-1A		p34-Arc		WDR-1	
	Log 2 (FC)	*p*	Log 2 (FC)	*p*	Log 2 (FC)	*p*
GSE1456	3.07	0.003	0.73	0.047	0.672	0.022
GSE2034	3.39	0.002	1.04	0.013	−0.039	0.865
GSE3193	1.02	0.001	0.60	0.024	0.377	0.131
GSE3494	2.11	0.024	0.89	0.024		

Four gene expression datasets were downloaded from the GEO database and analyzed as described in the text. Log 2-transformed values of fold change and *p*-values (*t*-test) were computed by comparative analysis between breast cancer tissues and normal tissues.

3.5 Immunoblot confirms upregulation of p34-Arc and coronin-1A in breast cancer tissue

Since the mRNA level of Wdr1 did not change significantly in the above-mentioned microarray analysis, and since there was no specific antibody available for this protein, Wdr1 was excluded from all further validation studies. In contrast, the differential expression of coronin-1A and p34-Arc in tumor tissues of breast cancer was validated by Western blot analysis using 11 pairs of matched tumor and nontumor tissue samples (Table 1). Almost all the tumor samples showed higher expression levels of coronin-1A compared to the paired nontumor samples (Fig. 3A). Expression levels of p34-Arc were also higher in tumor tissue samples than the nontumor samples. Although there were some variations between individuals in the amounts of coronin-1A and p34-Arc, both proteins were significantly upregulated in tumor tissues compared to nontumor populations (Fig. 3B). The band intensity ratios of coronin-1A and p34-Arc relative to β-actin were 0.66 ± 0.22 in nontumor tissues and 5.7 ± 1.8 in tumor tissues ($p = 0.02$), and 1.4 ± 0.5 in nontumor tissues and 6.5 ± 1.6 in tumor tissues ($p = 0.01$), respectively.

3.6 Coronin-1A and p34-Arc stimulates cell invasion of breast cancer cells

Arp2/3 complex is localized to lamellipodia and pseudopodia and essential for lamellipodia protrusion [37, 38]. Cell

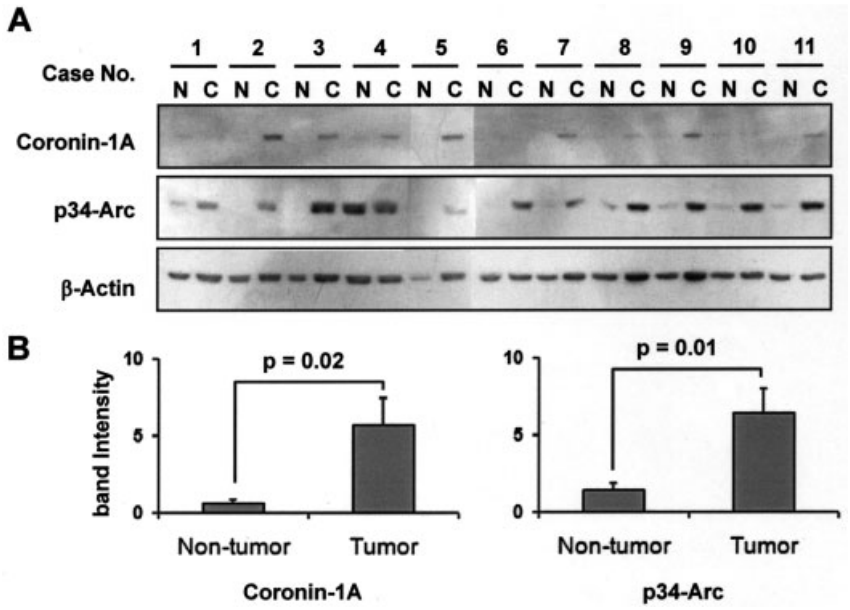

Figure 3. (A) Western blot analysis of coronin-1A and p34-Arc in 11 pairs of tumor and matched nontumor tissues of breast cancer. Case numbers are indicated in Table 1. (B) Averages of band intensities of coronin-1A and p34-Arc relative to β-actin ($N = 11$). Bar, SEM. Statistically significant differences ($p < 0.05$) are shown by paired *t*-test.

migration is initiated by plasma membrane protrusions [39]. An imbalance of F-actin assembly/disassembly may be responsible for the invasive potential of human carcinomas. We tested whether the upregulation of p34-Arc and coronin-1A in the tumor tissue of breast cancer was related to the invasive activity of breast cancer cells by *in vitro* invasion assays. The breast cancer cell lines, MCF7, Hs578T, MDA-MB-231, SK-BR-3, and ZR-75-1 were tested for the expression of p34-Arc and coronin-1A (Fig. 4A). While all the cell lines tested showed high expression levels of p34-Arc, only SK-BR-3 displayed a high expression level of coronin-1A. Hs578T showed a low expression level of coronin-1A, but this was undetectable in the other cell lines.

Accordingly, SK-BR-3 was selected for the cell invasion assays. Its ability to invade through a Matrigel-coated porous filter was significantly decreased by the siRNA knockdown of p34-Arc (Figs. 4B and C). The number of cells that migrated through the Matrigel-coated filter was reduced to less than 40% in the presence of 10–200 nM siRNA. On the contrary, a moderate overexpression of coronin-1A increased the invasive activity of SK-BR-3 (Figs. 4D and E). The results obtained showed that p34-Arc and coronin-1A played an important role in migration and invasion of breast cancer cells. The dynamic association and dissociation of such actin-remodeling proteins might exert a functional role for cell–substratum and cell–cell adhesions, which affect cell migration and invasion.

4 Conclusions

We applied proteomic techniques to protein expression profiling between tumor and nontumor tissues of breast cancer. A comparative analysis of the human breast tissue proteome by 2-D DIGE in combination with MS or MS/MS enabled us to identify 53 proteins that showed significant changes in expression levels. Among the upregulated proteins, coronin-1A, p34-Arc, and Wdr1, which contain consecutive WD-repeat motifs at their N-termini, are concerned with actin remodeling [25–27]. The upregulation of coronin-1A and p34-Arc levels was consistent with the increase in gene expression. Thus, it is suggested that the expression of the genes responsible for actin remodeling is required during cancer development. In fact, knockdown of p34-Arc or overexpression of coronin-1A in SK-BR-3 breast cancer cell line affected cell migration, when assessed by *in vitro* invasion assays.

In this study, we developed a simple method to analyze breast cancer tissues and this involved the removal of high abundant serum proteins followed by 2-DE within a narrow p*I* range. Many proteomic studies with breast tissues have been challenged by heterogeneous populations of cells present in human breast tumor tissues and blood vessels. For example, in the nontumor samples cellular proteins are less abundant than serum proteins, not only due to the absence of neoplastic cells, but also by the reduction of mammary gland parenchyma, especially in post-menopausal women. LCM can be applied to obtain relatively homogeneous cell populations [8, 9]. In spite of such an advantage, however, LCM provides only a limited amount of tissue sample. The method we used in the present study was not capable of providing an elaborative sample preparation like that of LCM, but is advantageous in experiments when the sample amount is limited. The expression patterns of several proteins such as catalase, $NADP^+$-dependent cytoplasmic isocitrate dehydrogenase, cytoplasmic malate dehydrogenase, and moesin between tumor and nontumor tissue samples

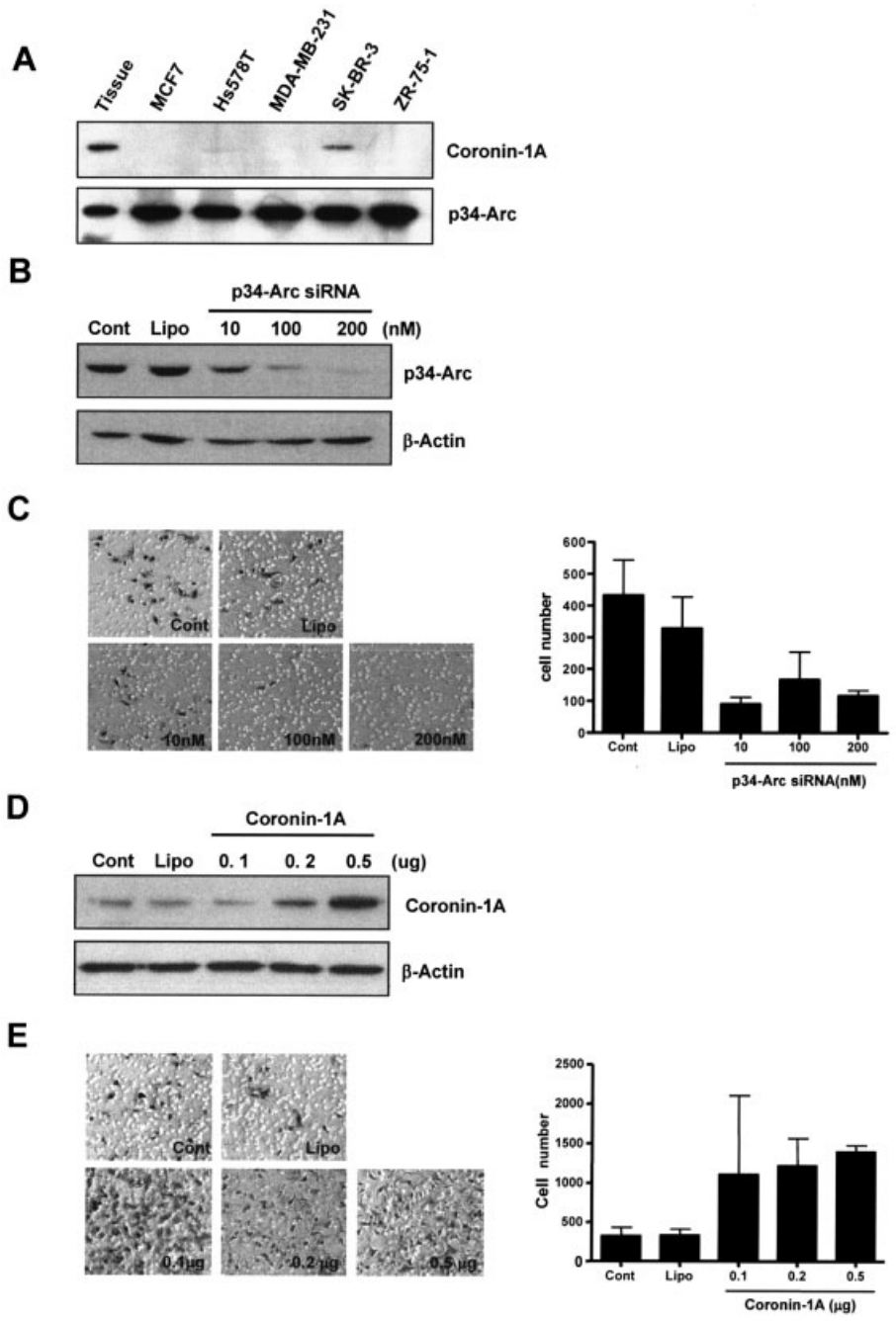

Figure 4. (A) Western blot analysis of coronin-1A and p34-Arc in a breast cancer tissue (positive control) and various breast cancer cell lines. (B) Knockdown of p34-Arc in SK-BR3 cell line at various concentrations of siRNA. At 72 h after transfection, cells were harvested and the expression level of p34-Arc was assessed by Western blot analysis using anti-p34-Arc antobody. β-Actin was used as a control. (C) The transwell assays were carried out to measure the invasive potential of SK-BR-3 cells treated with siRNA directed against p34-Arc. At 16 h after incubation of cells (initial cell number, 8×10^4) in the upper chamber, the cell number that migrated through Matrigel-coated filter was counted under microscopy with HE staining. Averages from three independent experiments are shown (mean ± SD). (D) Overexpression of coronin-1A in SK-BR3 cells transfected by plasmid pCNS-D2 containing coronin-1A gene. After 24 h of incubation, cells were harvested and used for Western blot analysis. (E) The transwell assays were carried out as described above at 24 h after transfection with coronin-1A plasmid.

were reliably comparable to previous reports [14–16, 18–20], showing that our method is useful and applicable for the comparative and quantitative analysis of breast cancer tissues. Immunodepletion, while allowing for the enrichment of low-abundance-proteins, can also inevitably remove sets of other interesting proteins. A strategy to deal with this problem will be required in future studies that involve an extended pH range.

Our findings of coronin-1A and p34-Arc, which are increased in breast tumor tissues, supports the emerging links between actin remodeling and breast cancer development. Such proteins are not only involved in actin polymerization/depolymerization, but are also related to the invasion and migration of malignant tumor cells, which may be prerequisite for breast cancer development and possibly for lymph node metastasis. Understanding the regulation of actin remodeling proteins such as coronin-1A and p34-Arc will provide new insights into the detection and management of breast cancer.

This study was supported by the grants (FPR08A2-090, FPR08A1-030, and FPR08A2-080) from the Functional Proteomics Center of the 21st Century Frontier R&D Program funded by the Korean Ministry of Education, Science and Technology, Republic of Korea.

The authors have declared no conflict of interest.

5 References

[1] Veronesi, U., Boyle, P., Goldhirsch, A., Orecchia, R., Viale, G., Breast cancer. *Lancet* 2005, *365*, 1727–1741.

[2] White, S. L., Gharbi, S., Bertani, M. F., Chan, H. L. *et al.*, Cellular responses to ErbB-2 overexpression in human mammary luminal epithelial cells: Comparison of mRNA and protein expression. *Br. J. Cancer* 2004, *90*, 173–181.

[3] Bertucci, F., Birnbaum, D., Goncalves, A., Proteomics of breast cancer: Principles and potential clinical applications. *Mol. Cell. Proteomics* 2006, *5*, 1772–1786.

[4] Smith, L., Lind, M. J., Welham, K. J., Cawkwell, L., Cancer proteomics and its application to discovery of therapy response markers in human cancer. *Cancer* 2006, *107*, 232–241.

[5] Alban, A., David, S. O., Bjorkesten, L., Andersson, C. *et al.*, A novel experimental design for comparative two-dimensional gel analysis: Two-dimensional difference gel electrophoresis incorporating a pooled internal standard. *Proteomics* 2003, *3*, 36–44.

[6] Tonge, R., Shaw, J., Middleton, B., Rowlinson, R. *et al.*, Validation and development of fluorescence two-dimensional differential gel electrophoresis proteomics technology. *Proteomics* 2001, *1*, 377–396.

[7] Boudreau, N., Myers, C., Breast cancer-induced angiogenesis: Multiple mechanisms and the role of the microenvironment. *Breast Cancer Res.* 2003, *5*, 140–146.

[8] Zang, L., Palmer Toy, D., Hancock, W. S., Sgroi, D. C., Karger, B. L., Proteomic analysis of ductal carcinoma of the breast using laser capture microdissection, LC-MS, and $^{16}O/^{18}O$ isotopic labeling. *J. Proteome Res.* 2004, *3*, 604–612.

[9] Zhang, D., Tai, L. K., Wong, L. L., Chiu, L. L. *et al.*, Proteomic study reveals that proteins involved in metabolic and detoxification pathways are highly expressed in HER-2/neu-positive breast cancer. *Mol. Cell. Proteomics* 2005, *4*, 1686–1696.

[10] Lee, J. E., Kim, H. J., Bae, J. Y., Kim, S. W. *et al.*, Neogenin expression may be inversely correlated to the tumorigenicity of human breast cancer. *BMC Cancer* 2005, *5*, 154.

[11] Chang, J. W., Kang, U.-B., Kim, D. H., Yi, J. K. *et al.*, Identification of circulating endorepellin LG3 fragment: Potential use as a serological biomarker for breast cancer. *Proteomics Clin. Appl.* 2008, *2*, 23–32.

[12] Friedman, D. B., Quantitative proteomics for two-dimensional gels using difference gel electrophoresis. *Methods Mol. Biol.* 2007, *367*, 219–239.

[13] Ryu, M. J., Kim, D., Kang, U. B., Kim, J. *et al.*, Proteomic analysis of γ-butyrolactone-treated mouse thalamus reveals dysregulated proteins upon absence seizure. *J. Neurochem.* 2007, *102*, 646–656.

[14] Tas, F., Hansel, H., Belce, A., Ilvan, S. *et al.*, Oxidative stress in breast cancer. *Med. Oncol.* 2005, *22*, 11–15.

[15] Balinsky, D., Platz, C. E., Lewis, J. W., Isozyme patterns of normal, benign, and malignant human breast tissues. *Cancer Res.* 1983, *43*, 5895–5901.

[16] Florianczyk, B., Pasternak, K., Grzybowska, L., Peszynski, J., Activity of isocitrate dehydrogenase in breast cancer. *Pol. Merkur. Lekarski* 1997, *2*, 376–377.

[17] Wang, Y., He, Q. Y., Chen, H., Chiu, J. F., Synergistic effects of retinoic acid and tamoxifen on human breast cancer cells: Proteomic characterization. *Exp. Cell Res.* 2007, *313*, 357–368.

[18] Reinerova, M., Veselovska, Z., Ausch, C., Rosen, H. R., Immunosuppressive activity of lymphocyte mitogenesis by breast cancer-associated p43. *Neoplasma* 1996, *43*, 363–366.

[19] Laguens, G. E., Coronato, S., Spinelli, O., Laguens, R. P., Di Girolamo, W., Can breast cancer Hsp 27 (Heat Shock Protein 27000) expression influence axillary lymph node status? *Breast* 2001, *10*, 179–181.

[20] Carmeci, C., Thompson, D. A., Kuang, W. W., Lightdale, N. *et al.*, Moesin expression is associated with the estrogen receptor-negative breast cancer phenotype. *Surgery* 1998, *124*, 211–217.

[21] Le Naour, F., Misek, D. E., Krause, M. C., Deneux, L. *et al.*, Proteomics-based identification of RS/DJ-1 as a novel circulating tumor antigen in breast cancer. *Clin. Cancer Res.* 2001, *7*, 3328–3335.

[22] Ono, S., Regulation of actin filament dynamics by actin depolymerizing factor/cofilin and actin-interacting protein 1: New blades for twisted filaments. *Biochemistry* 2003, *42*, 13363–13370.

[23] Goldberg, D. J., Foley, M. S., Tang, D., Grabham, P. W., Recruitment of the Arp2/3 complex and mena for the stimulation of actin polymerization in growth cones by nerve growth factor. *J. Neurosci. Res.* 2000, *60*, 458–467.

[24] Goley, E. D., Welch, M. D., The ARP2/3 complex: An actin nucleator comes of age. *Nat. Rev. Mol. Cell Biol.* 2006, *7*, 713–726.

[25] Lambrechts, A., Van Troys, M., Ampe, C., The actin cytoskeleton in normal and pathological cell motility. *Int. J. Biochem. Cell Biol.* 2004, *36*, 1890–1909.

[26] Uetrecht, A. C., Bear, J. E., Coronins: The return of the crown. *Trends Cell Biol.* 2006, *16*, 421–426.

[27] Rybakin, V., Clemen, C. S., Coronin proteins as multifunctional regulators of the cytoskeleton and membrane trafficking. *Bioessays* 2005, *27*, 625–632.

[28] Cai, L., Marshall, T. W., Uetrecht, A. C., Schafer, D. A., Bear, J. E., Coronin 1B coordinates Arp2/3 complex and cofilin activities at the leading edge. *Cell* 2007, *128*, 915–929.

[29] Honda, K., Yamada, T., Endo, R., Ino, Y. *et al.*, Actinin-4, a novel actin-bundling protein associated with cell motility and cancer invasion. *J. Cell Biol.* 1998, *140*, 1383–1393.

[30] Yamaguchi, H., Condeelis, J., Regulation of the actin cytoskeleton in cancer cell migration and invasion. *Biochim. Biophys. Acta* 2007, *1773*, 642–652.

[31] Chhabra, E. S., Higgs, H. N., The many faces of actin: Matching assembly factors with cellular structures. *Nat. Cell Biol.* 2007, *9*, 1110–1121.

[32] Pawitan, Y., Bjohle, J., Amler, L., Borg, A. L. *et al.*, Gene expression profiling spares early breast cancer patients

from adjuvant therapy: Derived and validated in two population-based cohorts. *Breast Cancer Res.* 2005, *7*, R953–R964.

[33] Wang, Y., Klijn, J. G., Zhang, Y., Sieuwerts, A. M. *et al.*, Gene-expression profiles to predict distant metastasis of lymph-node-negative primary breast cancer. *Lancet* 2005, *365*, 671–679.

[34] Sorlie, T., Perou, C. M., Tibshirani, R., Aas, T. *et al.*, Gene expression patterns of breast carcinomas distinguish tumor subclasses with clinical implications. *Proc. Natl. Acad. Sci. USA* 2001, *98*, 10869–10874.

[35] Miller, L. D., Smeds, J., George, J., Vega, V. B. *et al.*, An expression signature for p53 status in human breast cancer predicts mutation status, transcriptional effects, and patient survival. *Proc. Natl. Acad. Sci. USA* 2005, *102*, 13550–13555.

[36] Vaquerizas, J. M., Conde, L., Yankilevich, P., Cabezon, A. *et al.*, GEPAS, an experiment-oriented pipeline for the analysis of microarray gene expression data. *Nucleic Acids Res.* 2005, *33*, W616–W620.

[37] Machesky, L. M., Reeves, E., Wientjes, F., Mattheyse, F. J. *et al.*, Mammalian actin-related protein 2/3 complex localizes to regions of lamellipodial protrusion and is composed of evolutionarily conserved proteins. *Biochem. J.* 1997, *328*, 105–112.

[38] Bryce, N. S., Clark, E. S., Leysath, J. L., Currie, J. D. *et al.*, Cortactin promotes cell motility by enhancing lamellipodial persistence. *Curr. Biol.* 2005, *15*, 1276–1285.

[39] Pollard, T. D., Borisy, G. G., Cellular motility driven by assembly and disassembly of actin filaments. *Cell* 2003, *112*, 453–465.

